Magneto-optical study of excitonic binding energies, band offsets, and the role of interface potentials in $CdTe/Cd_{1-x}Mn_xTe$ multiple quantum wells

S. R. Jackson, J. E. Nicholls, W. E. Hagston, P. Harrison, T. Stirner, and J. H. C. Hogg
Department of Applied Physics, The University of Hull, Hull HU6 7RX, United Kingdom

B. Lunn and D. E. Ashenford
Department of Engineering Design and Manufacture, The University of Hull, Hull HU6 7RX, United Kingdom
(Received 21 January 1994)

Magneto-optical studies on a series of $CdTe/Cd_{1-x}Mn_xTe$ multiple-quantum-well structures with $x \simeq 0.08$ have identified the $1S$ and $2S$ states of both the light- and heavy-hole $n=1$ excitons. This has allowed changes of the exciton binding energies to be studied as a function of the depth of the confining potentials, which were tuned through the sp^3-d exchange interaction in the barrier layers by application of a magnetic field. Calculations of these binding energies by a variational technique are in general agreement with the observations. The exchange-induced splitting of the heavy-hole exciton is found to be consistent with between 0.35 and 0.45 of the band offset being in the valence band, which accounts for the absence of any evidence that the valence-band structure changes from a type-I structure to a type-II structure above a certain value of a magnetic field. However, this offset is found to be too large to account for the exchange-induced splitting of the light-hole exciton, which appears to be anomalously large. Calculations have shown that this anomaly cannot be explained in terms of the diffusion of Mn ions from the barrier regions into the wells. An alternative explanation is given in terms of field-dependent interface potentials wherein the sp^3-d exchange interaction is considered to be different in the interface regions of the multiple quantum wells to that in the barrier regions.

I. INTRODUCTION

The binding energies of free excitons in bulk II-VI compounds are relatively large compared with their counterparts in the III-V compounds. For example, the binding energies range from 10 meV in CdTe to 40 meV in ZnS,[1] compared with, for example, 4.2 meV in GaAs.[2] In quasi-two-dimensional quantum-well systems these values can, in principle, be enhanced up to a factor of 4, although significantly smaller enhancements are observed in practice since the confinement is never two dimensional. This enhancement of the exciton binding energy in quantum-well systems can play an important role in devices where it may be necessary for the exciton binding energy to exceed the LO phonon energy for efficient room-temperature device operation to be achieved. Magnetic multiple-quantum-well (MQW) systems allow the enhancement of exciton binding energies to be investigated in a way that is not possible in a nonmagnetic structure. The large sp^3-d exchange interaction that exists between the carriers and the magnetic ions allows considerable tuning, at low temperatures, of the band edges of a dilute magnetic semiconductor such as $CdTe/Cd_{1-x}Mn_xTe$ via the application of a magnetic field. Thus changes in the exciton binding energies can be investigated, and values of the conduction- and valence-band offsets determined.

In the present work a series of MQW $CdTe/Cd_{1-x}Mn_xTe$ samples with different well and barrier widths was investigated. The series had Mn ion concentrations with x between 0.06 and 0.08. Thin structures with 15 QW's were grown to ensure pseudomorphic growth; thus the strains in the samples were well defined. The excitonic lines from these structures were typically 1 meV wide and showed structure in both photoluminescence (PL) and photoluminescence excitation (PLE) spectra. This allowed an investigation of the well-width fluctuations of these systems. Also, in many of the samples both the $1S$ and $2S$ states of the heavy-hole and light-hole excitons were observed and, in one particular quantum-well system, both of these states could be observed over a wide range of magnetic-field values both at 2 and 20 K. This gave a unique opportunity to investigate the $1S$ and $2S$ states of both the light- and heavy-hole excitons as a function of the barrier heights, which were varied by the application of a magnetic field. In particular, the magnitude of the binding energies and their variation with the field could be determined. The results showed that, in this sample, the binding energy of both the heavy-hole exciton and the light-hole exciton is, to within about ± 1 meV, relatively insensitive to changes of the barrier heights. Comparison of these results with calculations of the oscillator strengths and binding energies assuming perfect interfaces, enables interesting conclusions to be drawn concerning the nature of these interfaces and limits to be placed on the minimum fraction of the total offset that must be assigned to the valence band.

II. EXPERIMENTAL METHODS

Multiple quantum wells of $CdTe/Cd_{1-x}Mn_xTe$ were grown with a VG80H molecular-beam epitaxy (MBE) system on (001) InSb substrates at a temperature of 230 °C. The substrates were cleaned prior to growth with

500-eV Ar^+ ions and then thermally annealed to remove lattice damage.[3] A 0.1 μm buffer layer of CdTe was grown before the MQW stack. Since we were particularly concerned to have pseudomorphic structures, the MQW stacks were grown without thick $Cd_{1-x}Mn_xTe$ capping layers. A series of samples with different well and barrier thicknesses was grown. Here we concentrate, principally, on only two, sample 1 and sample 2. The structures had 15 wells of CdTe and $Cd_{1-x}Mn_xTe$ barriers, with the top and bottom barriers of the same thickness as those of the stack. Both of these structures were of exceptionally good quality as judged by the PL and double-crystal x-ray-diffraction (DCXRD) line widths and, of particular relevance here, showed the 2*S* states of both light- and heavy-hole excitons.

X-ray diffraction spectra were recorded using a Bede double-axis diffractometer fitted with a double-bounce beam conditioner and a silicon monochromator to minimize the beam divergence and wavelength spread.

PL and PLE spectroscopy were carried out with the samples mounted strain-free in a superconducting magnet system in the Faraday configuration. The samples could be either immersed in overpumped liquid helium or raised to higher temperatures in an exchange gas. The samples were excited with laser irradiation, either from an Ar^+-ion laser or from a dye laser operating with pyridine 2. The emission was detected with a GaAs photomultiplier after being dispersed with a 1-m monochromator.

III. EXPERIMENTAL RESULTS

DCXRD of all the MQW samples showed clear satellite structure, usually out to the third order, and were close to that calculated using the dynamical theory of x-ray diffraction assuming an ideal structure with abrupt interfaces. This was particularly so for sample 1, Fig. 1, where the spectrum shows, in addition to the main satellite reflections, very detailed Pendellosung short-period thickness fringes. The spacing of these fringes, which are visible to high-order numbers, enables a very accurate determination of the corresponding layer thicknesses within the structure to be made, and the fact that the fringes are so clearly defined indicates that these layer thicknesses are exceptionally uniform across the x-ray-beam footprint. For sample 1 the structure was found to be pseudomorphic to the substrate, with a manganese concentration of 0.075, and to have well and barrier widths of 75 and 158 Å. Sample 2, which showed some broadening of the rocking curve from the ideal, was found to be partially relaxed and had a manganese concentration of 0.077 with well and barrier widths of 52 and 176 Å. The relaxation was 100% for the CdTe layers and 60% for the $Cd_{1-x}Mn_xTe$ barrier layers. The results for both samples for the well and barrier widths are in the range expected from the molecular-beam fluxes. The whole series of MQW samples, such as sample 1 and sample 2, has rocking curves which show, to a greater or lesser extent, a modulation of the Pendellosung fringes relating to a characteristic length of $\simeq 1000$ Å. This modulation arises from an enhancement of the thickness fringes from the CdTe buffer layer caused by a phase shift introduced between the wave fields scattered from the substrate and the buffer by a thin 14 Å layer of heavily mismatched material at the substrate interface. Layers of In_2Te_3 have been previously identified by Raman spectroscopy[4] at InSb/CdTe heterojunction interfaces and hence we attribute the interface layer to this same origin in our structures.

The PL and PLE spectra of sample 1, are shown in Fig. 2. The PL, excited with 100 mW/mm^2 of 488 nm radiation, shows emission bands that are blueshifted, through confinement, by about 25 meV from the CdTe band edge. The higher-energy pair of lines around 7653 Å are attributed to free exciton emission (e_1h_1) involving heavy holes (see below). The broader emission of 7667 Å is

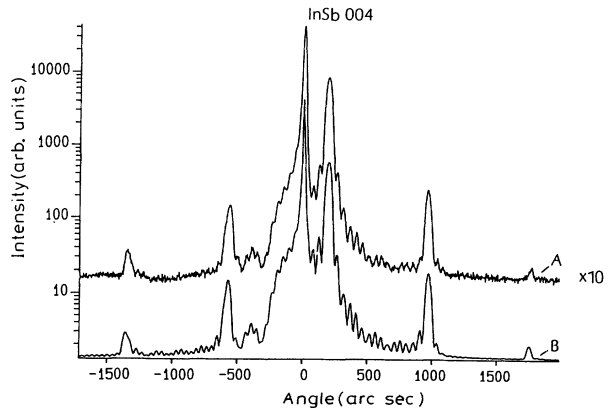

FIG. 1. Recorded DCXRD of a $CdTe/Cd_{1-x}Mn_xTe$ MQW, sample 1, with 15 quantum wells, *A*. Dynamical simulation of the spectrum, *B*. The simulation is consistent with the structural details of this sample given in Table I and with there being a thin In_2Te_3 layer of 14 Å thickness between the CdTe buffer layer and the InSb substrate.

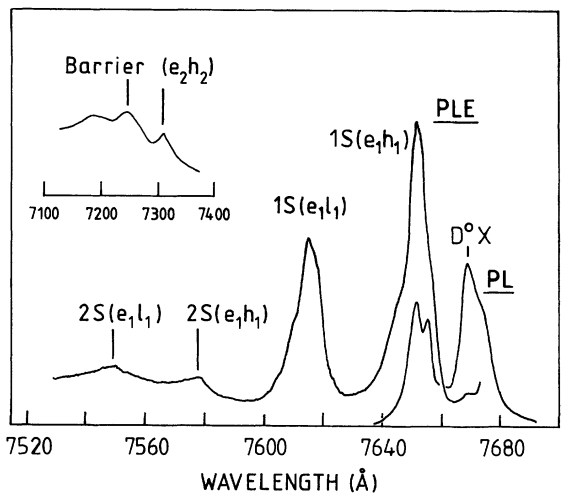

FIG. 2. Photoluminescence (PL) and photoluminescence excitation (PLE) spectrum recorded from $CdTe/Cd_{1-x}Mn_xTe$ MQW, sample 1, see Table I. The PL was excited with 488 nm radiation; the PLE was monitored on the D^0X emission. The 1*S* and 2*S* refer to the $n=1$ and 2 states of the light-hole (e_1l_1) and heavy-hole (e_1h_1) excitons.

shifted from the (e_1h_1) emission to longer wavelengths by 3.5 meV. Comparison with the emissions of bulk CdTe (Ref. 5) allows it to be assigned to the recombination of donor-bound excitons D^0X. The intrinsic nature of the D^0X emission was confirmed by checking its nonlinear behavior at higher excitation powers. The double peak observed in the (e_1h_1) transition is attributed to interface roughness and is discussed in more detail later. The temperature-dependent behavior of these lines and of the D^0X emission is shown in Fig. 3.

PLE spectra were recorded while monitoring the D^0X emission. In Fig. 2, the lowest-energy excitation peak resonance at 7651 Å coincides with the higher-energy PL peak from the (e_1h_1) exciton. Calculations based on the envelope-function approximation (described in more detail below) were carried out to obtain energies of the various quantum states of the system with allowance made for strain shifts[6] of the band edges appropriate to pseudomorphic growth, as shown by DCXRD for this sample. On the basis of these calculations the transitions around 7653 and 7613 Å can be assigned to the heavy-hole (e_1h_1) and the light-hole (e_1l_1) excitons, respectively. Likewise the two resonances at 7309 and 7240 Å can be attributed, respectively, to the (e_2h_2) transition and an excitonic transition in the barrier layers. The reason for making this "barrierlike" assignment is that its energy position corresponds to free excitons in $Cd_{1-x}Mn_xTe$ with a manganese concentration of 0.075,[7] which is very close to that determined by DCXRD. Also its large Zeeman splitting, see below, is consistent with this assignment. The PL and PLE data for sample 2 were of a similar quality to that of sample 1 but a greater blueshift of the quantum-well transitions was observed, as appropriate to a narrower well. The energies of the various transition of the two samples are shown in Table I.

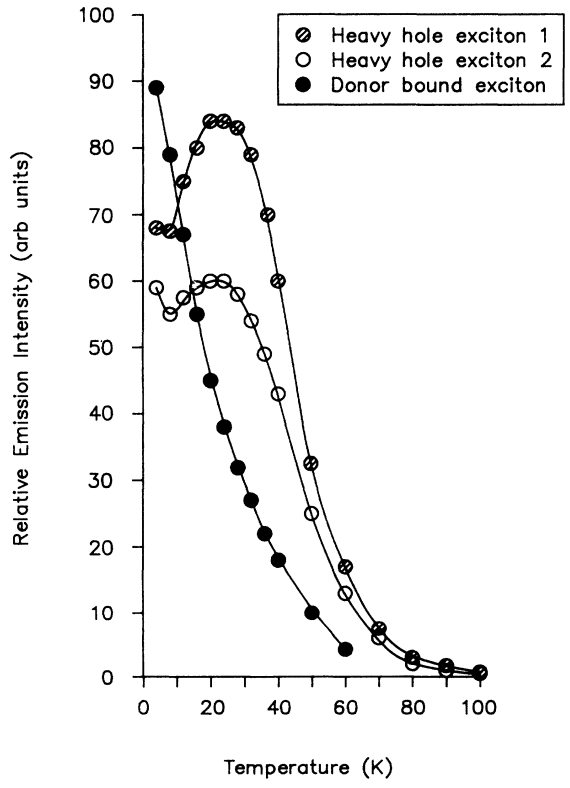

FIG. 3. Temperature dependence of the PL intensity of the transitions observed in Fig. 2. The two heavy-hole excitons referred to as 1 and 2 correspond to the shorter and longer wavelength peaks seen in Fig. 2 around 7653 Å, which arise from well-width fluctuations.

In a magnetic field applied in the Faraday configuration the various transitions split into σ^+ and σ^- polarized components with almost 100% polarization. The splitting is shown in Fig. 4 for sample 1 for the quantum-well states. For both samples the overall splitting pattern of the barrierlike resonances is in close agreement with that expected for $Cd_{1-x}Mn_xTe$ barriers having the compositions of Table I. For example, the behavior of the barrier resonances for sample 2 is shown in Fig. 5. The fit to the data is made assuming the conduction- and valence-band edges follow the modified Brillouin function,[8]

$$\Delta E_{c[v]} = N_0\alpha[N_0\beta]xS(x)B_j\left[\frac{g\mu_B S_0 B}{k[T(x)+T_0(x)]}\right], \quad (1)$$

with values of the exchange constants $(N_0\alpha)$ and $(N_0\beta)$ equal to 220 and 880 meV, respectively, with $x=0.078$ and with values of the phenomenological parameters, which account for antiferromagnetic pairing, $S_0=1.3$ and $T_0=3.1$ K. These values are close to those observed for bulk material[8] for this manganese concentration and allows us to conclude that the behavior of the thin magnetic barrier layers, of thickness ≈ 150 Å, are essentially bulklike. Similar remarks apply to the barrierlike resonances in sample 1, although in this case the light-hole resonances were not so well defined at all values of the magnetic field.

The magnetic behavior of the light- and heavy-hole exciton states of the well, which we denote as $(e_1h_1)^{\pm}$ and $(e_1l_1)^{\pm}$ from here on, are shown in Fig. 4 for sample 1. The magnetic splittings of both states are similar, but of

TABLE I. Structural and optical parameters of the two multiple quantum wells that are described in detail throughout this work. $E(el)$ [$E(eh)$] refers to the light- (heavy-) hole exciton energy in the barrier B, or the $1S$ or $2S$ states of the quantum well.

	Sample 1	Sample 2
Magnetic ion concentration	0.075	0.078
Well width (Å)	72	52
Barrier width (Å)	156	159
Strain in well ($\times 10^{-3}$)	−1.03	−0.96
Strain in barrier ($\times 10^{-3}$)	+0.66	+0.72
$E(eh)_B$ (meV)	1712.6	1713.8
$E(el)_B$ (meV)	1705.9	1713.8
$E(e_1h_1)_{1S}$ (meV)	1620.2	1634.5
$E(e_1h_1)_{2S}$ (meV)	1636.2	1652.2
$E(e_1l_1)_{1S}$ (meV)	1628.2	1643.2
$E(e_1l_1)_{2S}$ (meV)	1642.5	1657.7

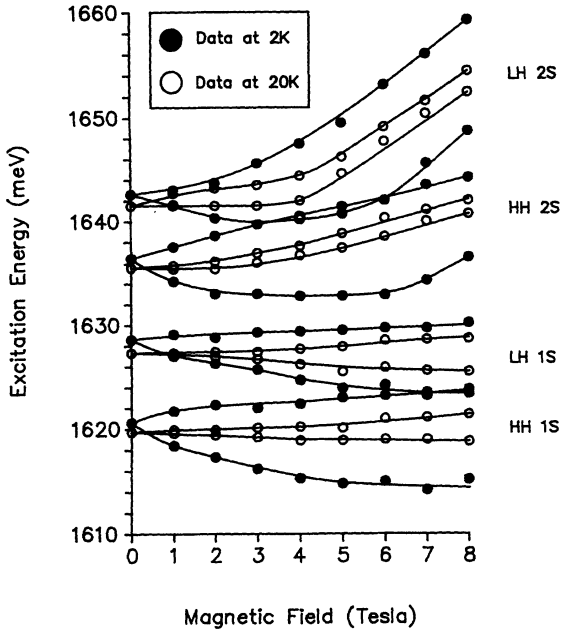

FIG. 4. Exchange-induced splittings in the Faraday configurations (B parallel to growth axis) of the $1S$ and $2S$ states of the light-hole (LH) and the heavy-hole (HH) excitons, recorded at 2 and 20 K for sample 1.

particular note is the diamagnetic behavior of the two upper resonances, observed at 7579 and 7547 Å in zero field. From their pronounced diamagnetic behavior these transitions are attributed to the $2S$ states of the (e_1h_1) and (e_1l_1) excitons, respectively. Figure 4 also shows the splitting of the different transitions when the sample temperature is raised to 20 K. At this temperature thermal effects cause the exchange splitting to be significantly reduced and the diamagnetic behavior of the $2S$ states is more apparent. For sample 2, the $2S$ state of the (e_1l_1) exciton was less distinct and could not be observed at the higher temperature. Thus the (e_1l_1) data could not be corrected for the diamagnetic behavior as was done for sample 1. Consequently the analysis below is based mainly on sample 1. Figure 6 shows the energy difference between the $1S$ and $2S$ states of the (e_1h_1) and (e_1l_1) excitons for a range of MQW's with different well widths.

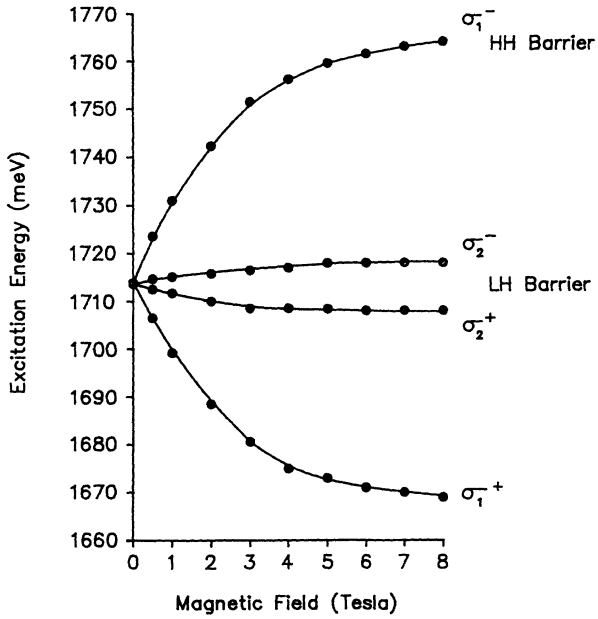

FIG. 5. Exchange-induced splittings of the $Cd_{1-x}Mn_xTe$ barrier states for sample 2 at 2 K. A similar splitting of the heavy-hole states was observed for sample 1, but the light-hole states were not so well defined at all field values. Note that the optical linewidths are too large to resolve the LH and HH excitons at zero field caused by the strain shown in Table I.

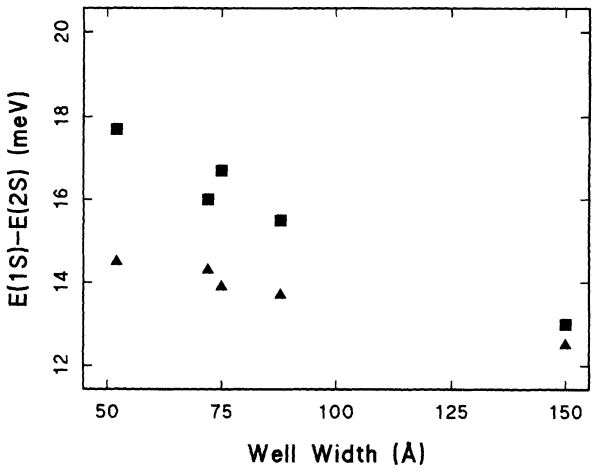

FIG. 6. Variation of the energy difference between the $1S$ and $2S$ states of the (e_1h_1) and (e_1l_1) excitons at zero magnetic field for different samples, as a function of well width. Values of the Mn concentration of the barriers and the barrier width of the different samples are, reading from the narrow to wide wells, 0.078, 159 Å (sample 2); 0.077, 156 Å (sample 1); 0.079, 150 Å (sample 3); 0.078, 173 Å (sample 4); and 0.047, 150 Å (sample 5). ■ and ▲ refer to the (e_1h_1) and (e_1l_1) excitons, respectively.

Confirmation of the identity of the (e_1h_1) and (e_1l_1) states was made by investigating the magnetic-field-induced splitting of the states with the sample in the Voigt geometry, with the magnetic field parallel to the plane of the layers and perpendicular to both the incident exciting light and the emission. The magnetic-field-induced splitting for sample 1 is shown in Fig. 7. The smaller splitting of both $1S$ and $2S$ (e_1h_1) states in this

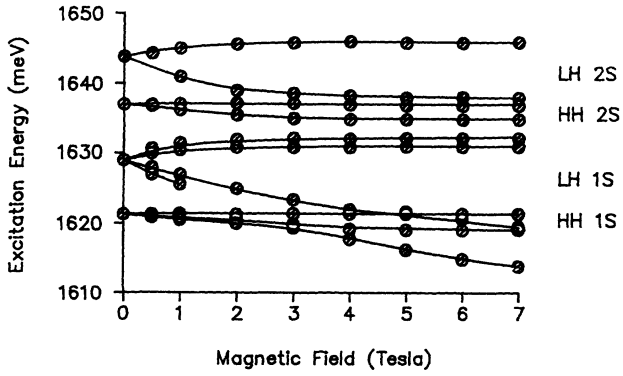

FIG. 7. Exchange-induced splittings in the Voigt configuration (B perpendicular to growth axis) of the $1S$ and $2S$ states of the light-hole (LH) and heavy-hole (HH) excitons, recorded at 2 K for sample 1.

geometry and the larger splitting of both $1S$ and $2S$ (e_1l_1) states confirms the identity of the states[9] and also serves to correlate the corresponding $2S$ state with its respective $1S$ state.

IV. DISCUSSION

A. Interface roughness

The fine structure observed in Fig. 2 on the (e_1h_1) transitions in both PL and PLE, together with a similar but less-well-resolved structure in the (e_1l_1) PLE transition, indicates the extent of well-width fluctuations in these $CdTe/Cd_{1-x}Mn_xTe$ structures. First, we note that the separation between the (e_1h_1) peak in PLE and the shoulder at higher energy is ≈ 1.5 meV. For a quantum well of width 72 Å this energy corresponds to a well-width difference of almost exactly 1 ML ($\frac{1}{2}a_0$), based on the envelope-function approximation referred to above. Second, the separation between the peak and the low-energy shoulder corresponds to a well-width difference of about $\frac{1}{2}$ ML. These latter two transitions are seen much more distinctly as two peaks in the PL spectrum. Fluctuations such as these are readily explained from a consideration of the growth mechanism, where the number of atomic planes grown within a single layer need not correspond to an exact integer. Consequently, at the end of the growth of one layer, migration of atoms on the growth surface leads to island formation, which becomes fixed by growth of the next overlayer. This can occur at each interface when the manganese source is opened or closed. To account for distinct peaks in the PL and PLE data corresponding to either 1- or $\frac{1}{2}$-ML fluctuations requires island growth on a scale that is both greater than and less than the exciton diameter (which is calculated below to be ~ 140 Å), respectively. If we assume for simplicity that for small island size the average height of the interface fluctuation amounts to $\frac{1}{2}$ ML, then the structure observed in Fig. 2 can be accounted for if it is assumed that the interfaces have some regions of small-island-size growth and other regions of large-island-size growth, $\gtrsim 140$ Å. Comparison of the (e_1h_1) transitions observed in PL and PLE, Fig. 2, shows that the PL is relatively stronger from the wider parts of the wells. This is to be expected when intra-well-width fluctuations occur owing to rapid thermalization of the carriers to the wider parts (i.e., lower-energy regions). If inter-well-width fluctuations predominate, relaxation of carriers is not expected in this sample since the barriers are 150 Å thick, thus drastically limiting any tunneling processes. The temperature dependence of the (e_1h_1) emission, Fig. 3, from the wider regions of the wells also supports intralayer fluctuations as opposed to interlayer fluctuations. Above 10 K the (e_1h_1) emissions increase, in part owing to reduced trapping at the D^0X centers. However, increased thermalization of excitons into the narrower regions of the quantum well would increase the relative emission from this region, as observed. Such a thermalization effect is much less likely to occur if only interlayer fluctuations are present, since the barrier potentials for electrons and heavy holes in these samples is estimated to be ~ 75 and ~ 45 meV, respectively (see below), considerably greater than kT at the sample temperature in these measurements.

B. Type-II transition

Deleporte *et al.*[10] have reported a magnetic-field-induced type-I to type-II transition in a $CdTe/Cd_{1-x}Mn_xTe$ system with similar structural parameters to those of our own samples (with the exception that the former was grown on ⟨111⟩ GaAs). In order to assess whether such a transition is possible in our samples, we note that for a $CdTe/Cd_{1-x}Mn_xTe$ MQW system with $x \simeq 0.075$ the total band offset is ~ 120 meV. At a field of 8 T applied along the growth direction, the confining potential of one of the heavy-hole components is reduced by ~ 40 meV. Thus if the partition ratio, defined here as the valence-band offset to the total band offset, of the $CdTe/Cd_{1-x}Mn_xTe$ system is less than about 0.35, the system would exhibit a field-induced type-I to type-II transition for this heavy-hole component. Conversely, if no such transition is observed, the partition ratio must be greater than 0.35 (this conclusion is modified slightly if allowance is made for the Coulomb attraction of the electron and hole, see below).

To quantify the significance of a type-II transition, we carried out detailed calculations, within the envelope-function approximation, of the binding energies and oscillator strengths of the relevant heavy-hole (e_1h_1) transitions in this transition region when the field is applied along the growth direction. Assuming a perfect MQW system we employed a variational technique (Hilton, Hagston, and Nicholls[11]) with a trial wave function

$$\Psi = \varphi_e(z_e)\varphi_h(z_h)\phi_R(r) ,$$

and Hamiltonian

$$H = H_e + H_h + H_{eh} ,$$

where φ_e and φ_h are the one-particle (uncorrelated) wave functions and ϕ_R describes the relative motion of the electron (e) and hole (h). For the $1S$ state we take

$$\phi_R = \exp\left[\frac{-r}{\lambda}\right] ,$$

and for the $2S$ state we take

$$\phi_R = \left[1-\frac{\alpha r}{\lambda}\right]\exp\left[\frac{-r}{\lambda}\right] ,$$

where r, the spatial coordinate, is given by

$$r^2 = (x_e-x_h)^2+(y_e-y_h)^2+(1-\beta^2)(z_e-z_h)^2 ,$$

and λ and β are variational parameters.

H_e and H_h, the one-particle Hamiltonians of the electron and hole, respectively, are given by

$$H_{e,(h)} = \frac{-h^2}{2m_{e(h)}}\frac{\partial^2}{\partial z^2} + V(z) .$$

The electron and hole interaction term H_{eh} includes the Coulombic term and the kinetic energy in the x-y plane

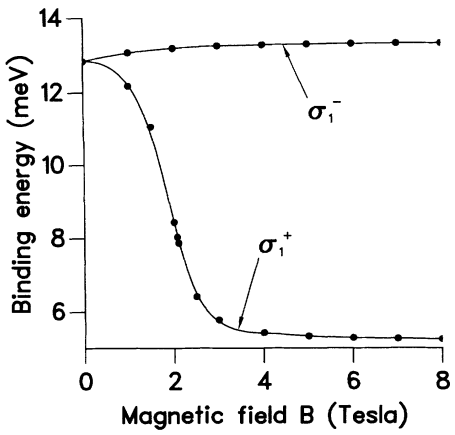

FIG. 8. Calculated variation of the binding energy of the 1S states of the $(e_1h_1)^{\pm}$ excitons of sample 1, assuming a partition ratio of 0.2.

and is represented by

$$H_{eh}=\frac{p_\perp^2}{2\mu_\perp}-\frac{e^2}{\epsilon[r_\perp^2+(z_e-z_h)^2]^{1/2}}\ .$$

Figure 8 shows how the $(e_1h_1)^{\pm}$ exciton binding energies for a MQW sample with the structural parameters of sample 1 are expected to change with magnetic field for a partition ratio 0.2. At zero field the (e_1h_1) exciton binding energy is calculated as 12.8 meV. The effective well depths of the electron (and hole) vary with the strength of the applied magnetic field. For one spin component of the electron (or hole) the well depth increases by Δ_e (Δ_h), whereas for the other spin component it decreases by the same amount Δ_e (Δ_h). The value of Δ_e (Δ_h) can readily be deduced, for a given choice of partition ratio, from the expression in Eq. (1). Having determined the confining potential for each spin component of the electron (and hole) in the presence of the magnetic field, the corresponding value of the one-electron energy and one-electron wave function $\varphi_e(z_e)$ [$\varphi_h(z_h)$] is calculated. The parameters λ, α, and β are then varied to maximize the exciton binding energy for the associated excitonic component. In this manner the exciton binding energy and the total exciton energy can be calculated at each value of the magnetic field. These calculations show that in an applied field the electron and hole involved in the $(e_1h_1)^-$ exciton experience increased well depths, and a resulting slight increase in the binding energy, which can be attributed to the increase in localization of the one-particle wave functions. As opposed to this, the electron and hole involved in the $(e_1h_1)^+$ exciton experience decreased well depths until eventually the valence band across the MQW would become flat and then turn type II at a field of 2.1 T. It can be seen that the binding energy would fall rapidly before the transition to a type-II region is reached, and then would continue to fall thereafter, eventually leveling off around 5 meV for a type-II band lineup. The transition point can be roughly identified as the point of inflexion on this curve. (When the valence band first becomes flat, the residual interaction between the electron and hole prevents the system going immediately into the type-II regime. Detailed calculation shows that this does not alter significantly the previous conclusions, the main effect being to change the transition point to slightly larger values of the magnetic field $\lesssim 2.5$.) Figure 9 shows the expected effect of the magnetic field upon the heavy-hole 2S excitons. The form of the curves is almost identical to that of the 1S binding energies although the absolute magnitudes are much smaller.

For the same partition ratio 0.2, the light-hole valence band would not become type II and the (e_1l_1) exciton binding energies would stay roughly constant at all fields. The (e_1l_1) exciton is calculated to have a zero-field binding energy of around 11.7 meV. For the $(e_1l_1)^-$ exciton this increases slowly up to 12.6 meV at 8 T, while for the $(e_1l_1)^+$ exciton the binding energy would decrease to 9.9 meV over the same field range.

Figure 10 shows how the $(e_1h_1)^{\pm}$ exciton emission energies would change if the partition ratio were 0.2. The initial splittings are roughly symmetrical, but as the band lineup approaches type II for the $(e_1h_1)^+$ state there is a slight increase in energy to a local maximum at the transition point followed by a rapid fall thereafter, with the system firmly in the type-II regime. (The increase in the emission energy occurs because the decrease in the binding energy of the exciton is more rapid than the decrease in the single-particle energies.) Figure 11 shows how the oscillator strength, evaluated using the technique described by Hilton *et al.*,[12] for both heavy-hole exciton transitions would change. While the oscillator strength of the $(e_1h_1)^-$ transition remains roughly constant the $(e_1h_1)^+$ transition rises slightly before falling a full order of magnitude beyond the transition point. This fall in the oscillator strength can be attributed to a reduction in the overlap integral between the electron and hole. As the valence-band offset shrinks, the hole becomes less localized in the CdTe well until eventually, in the type-II region, the hole becomes increasingly more localized in the $Cd_{1-x}Mn_xTe$ layer as the field increases still further.

Calculated values of the exciton binding energies and oscillator strengths change significantly with the partition

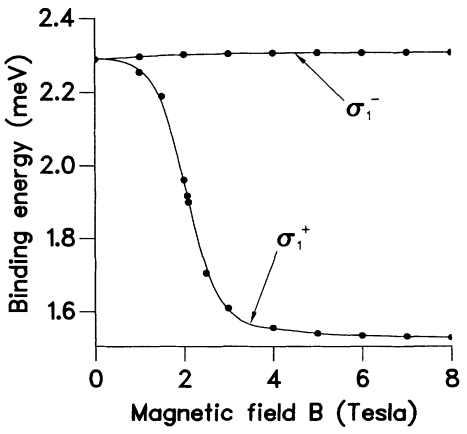

FIG. 9. Calculated variation of the binding energy for the 2S states of the $(e_1h_1)^{\pm}$ excitons of sample 1, assuming a partition ratio of 0.2.

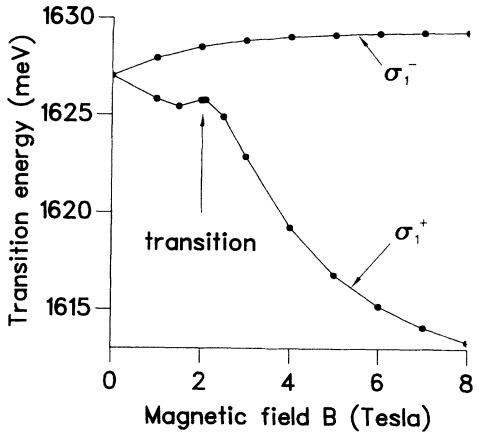

FIG. 10. Calculated variation of the transition energy of the 1S states of the $(e_1h_1)^{\pm}$ exciton for sample 1, assuming a partition ratio of 0.2.

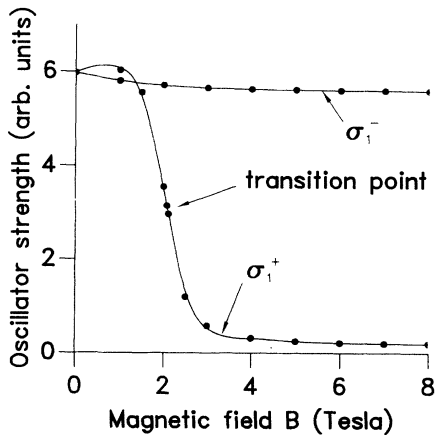

FIG. 11. Calculated variation of the oscillator strengths of the 1S states of the $(e_1h_1)^{\pm}$ excitons for sample 1, assuming a partition ratio of 0.2

ratio. For example, if the partition ratio were 0.4 then the valence band could not become type II in these samples. Our calculations then show that there is little change in the binding energies of any of the excitons as the magnetic field is increased. The essential results for the (e_1h_1) and (e_1l_1) exciton binding energies are gathered together in Table II for partition ratios of 0.2 and 0.4. In this connection we note that in order to avoid using the dielectric constant of CdTe the exciton binding energies were calculated in terms of the three-dimensional Rydberg constant, which for the heavy-hole exciton is 10 meV.[1] However, in the absence of the equivalent quantity for the light-hole exciton, we have scaled it from that of the heavy-hole exciton assuming the Luttinger parameters given by Dang, Neu, and Romestain.[13] This gives a value of 6.6 meV for the three-dimensional Rydberg constant. From these calculations we note that extensive examination of the experimental observations reveal none of the characteristic features expected if the samples investigated here were to have gone to type II. Having established that this is the case it is reasonable, given the limitations of the theory, to assume that the valence-band ratio is $\gtrsim 0.35$. With this to hand we consider other interesting features revealed by the experimental data.

C. Exciton binding energies

The observation of the 1S and 2S states of both (e_1h_1) and (e_1l_1) excitons over the whole magnetic-field range for sample 1 allows considerable information to be obtained about the heavy- and light-hole exciton binding energies from the 1S/2S energy separation, which at zero magnetic field are 16.0 and 14.3 meV, respectively. In an infinite potential well the ratio of the 1S/2S binding energies for a three-dimensional exciton is 4 while for a two-dimensional exciton this ratio increases to 9. In a finite QW the exciton is neither fully two nor three dimensional and this leads to uncertainty in establishing the binding energies of the 1S and 2S states. Taking a value for this ratio of 5, see Table II, gives binding energies of the 1S and 2S states to be 20.0 and 4.0 meV for the heavy-hole (HH) exciton and 17.9 and 3.6 meV for the light-hole (LH) exciton, respectively, with uncertainties of about ± 1.5 meV.

Figure 6 shows how the energy difference between the 1S and 2S (e_1h_1) and (e_1l_1) exciton states varies with well width. Although the samples referred to in Fig. 6 have somewhat different barrier widths and magnetic-ion concentrations, the figure shows two general trends. One is the increasing binding energies as the well width is narrowed, and the second is the slight larger binding energy

TABLE II. Calculated 1S and 2S binding energies (BE) in meV for both light- $(e_1l_1)^{\pm}$ and heavy-hole $(e_1h_1)^{\pm}$ excitons, together with the relative oscillator strengths (OS) of the heavy-hole transitions at different applied magnetic fields for two different partition ratios K, the fraction of the valence-band offset to the total-band offset at the heterojunction.

	$K=0.2$			$K=0.4$		
B (T)	0	4	8	0	4	8
BE $(e_1h_1)^+$ 1S(2S)	12.8(2.3)	5.6(1.6)	5.2(1.5)	12.8(2.3)	12.0(2.3)	11.4(2.2)
BE $(e_1h_1)^-$ 1S(2S)	12.8(2.3)	13.3(2.3)	13.3(2.3)	12.8(2.3)	13.1(2.3)	13.1(2.3)
BE $(e_1l_1)^+$ 1S(2S)	11.7(2.3)	10.2(2.2)	9.9(2.1)	12.8(2.4)	12.5(2.3)	12.4(2.3)
BE $(e_1l_1)^-$ 1S(2S)	11.7(2.3)	12.5(2.3)	12.6(2.3)	12.8(2.4)	12.9(2.4)	12.9(2.4)
OS $(e_1h_1)^+$ 1S	1.00	0.05	0.03	1.00	1.08	1.13
OS $(e_1h_1)^-$ 1S	1.00	0.94	0.93	1.00	0.99	0.99

of the (e_1h_1) exciton compared to the (e_1l_1) exciton. Such effects have already been predicted earlier by the authors.[14]

When a magnetic field is applied to the $CdTe/Cd_{1-x}Mn_xTe$ MQW's the strong sp^3-d exchange interaction[8] that exists between the carriers and the magnetic ions of the barrier layers change the effective band gaps of the latter and, hence, the confining potentials of the quantum well. Not only does this change the one-particle confinement energies of the electrons and holes in their respective wells, but it also changes both light- and heavy-hole exciton binding energies owing to changes in the overlap of the one-particle wave functions in the modified potential wells.

In Fig. 4 the magnetic splitting of the $1S$ and $2S$ states of the (e_1l_1) and (e_1h_1) excitons at 2 and 20 K were shown for sample 1. At the higher temperature the sp^3-d exchange energy is considerably less owing to the lowering of the spin ordering of the magnetic ions, and this manifests itself as a reduced magnetic-field splitting. By reducing the effect of the exchange interactions, the diamagnetic effects, which become more pronounced at higher fields, can be allowed for when calculating the energy difference between the appropriate $1S$ and $2S$ states. These energy differences are shown in Fig. 12, for the $(e_1l_1)^{\pm}$ and $(e_1h_1)^{\pm}$ excitons, after correction for diamagnetic efforts. Figure 12 implies that the change in the binding energy of the heavy-hole $(e_1h_1)^{\pm}$ excitons appears to be very small, less than about ∓ 0.5 meV. Such a small change seems at first sight surprising, particularly for the $(e_1h_1)^{+}$ exciton, since the heavy-hole potential well is reduced by ~ 40 meV in a field of 8 T. Conversely, for the $(e_1h_1)^{-}$ exciton the potential well is increased in the field by ~ 40 meV. Thus for a considerable change of the heavy-hole confining potential there appears to be little change in the exciton binding energy.

The binding energies of the $(e_1l_1)^{\pm}$ excitons change by about ∓ 2 meV in a field of 8 T, which, compared with that of the (e_1h_1) exciton, appear unusually large on two accounts. First, at a given magnetic field the change in barrier height of the light hole is only one-third that of the heavy hole; second, for the (e_1l_1) exciton, as the electron becomes more strongly localized with applied field, the light hole becomes less localized and vice versa, whereas for the (e_1h_1) exciton as the electron becomes more (or less) strongly localized so too does the heavy hole. There is some uncertainty in determining the $1S$ binding energy from a knowledge of the $1S$ to $2S$ energy difference, principally from correcting for the diamagnetic effects. We estimate the error these cause in the $1S$ binding energy to be about ± 1.5 meV. Thus, to within this experimental uncertainty the binding energies of the (e_1h_1) and (e_1l_1) excitons change very little with magnetic field and, in all probability, the binding-energy changes lie within the range ± 1 meV. The important point to note is that such small binding-energy changes again reinforce the argument that the system does not undergo a type-II transition. In this case a change similar to that shown in Fig. 8 would be expected, but clearly no such change is seen. However, the changes of binding energy are consistent with the theoretical calculations appropriate to a partition ratio of 0.4 (see Table II).

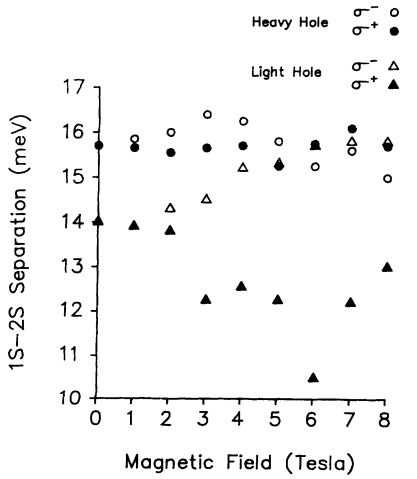

FIG. 12. Measured energy differences between the $1S$ and $2S$ states of the $(e_1h_1)^{\pm}$ excitons of sample 1 as a function of magnetic field. The data are taken from Fig. 4 after correction of diamagnetic effects.

The next major point concerns the actual magnitude of the binding energies. As is clear from Table II, the calculated values of the binding energies are appreciably smaller than the observed values. In relation to this we note that the calculations employ Luttinger parameters appropriate to bulk material, and an effective dielectric constant $\epsilon \sim 10.6$ (which is equivalent to a static dielectric constant). One or both of these assumptions can be changed. For example, the observed exciton binding energies are close to those of the LO phonon energy. It is well known[15] that in such a situation the use of the low-frequency (i.e., static) dielectric constant becomes questionable, and one should employ a frequency-dependent dielectric constant. A particularly simple choice here would be to replace the static dielectric constant $\epsilon \sim 10.6$ by the high-frequency value $\epsilon_\infty \sim 7.4$. With this choice it is found that the calculated exciton binding energies are then several meV larger than the observed values.

Agreement with the experimental values can be obtained by using ϵ_∞ and, for example, decreasing the Luttinger parameters from their bulk values. Alternatively, we could still employ the static dielectric constant and increase the theoretical values of the exciton binding energies by increasing the Luttinger parameters from their bulk values. Such procedures are *ad hoc*, and would seem to be of little value until such time as the effective mass parameters can actually be measured experimentally. However, the useful conclusions that can be drawn are that the binding energies are large (i.e., approaching the value of the LO phonon energy) and can only be accounted for theoretically if the Luttinger parameters are different in MWQ's from those reported by Dang, Neu, and Romestain[13] for bulk material, and/or a frequency-dependent dielectric constant is employed in the calculations.

D. Band offsets

The magneto-optical data described in Sec. III provide unique information for determining the partition ratio at

the $CdTe/Cd_{1-x}Mn_xTe$ heterojunction since they relate to three essentially independent measurements. These are the magnetic-field splittings of both the $(e_1l_1)^{\pm}$ and $(e_1h_1)^{\pm}$ transitions and the energy difference between these transitions at zero magnetic field. Each of these is dependent on the value of the partition ratio. Previous determinations of this ratio have usually been made from either the magnetic-field splitting of the $(e_1h_1)^{\pm}$ transitions or from the energy difference between the (e_1h_1) and (e_1l_1) transitions in zero field. These results are summarized in Fig. 13, where the absolute value of the valence-band offset is plotted against the manganese concentration of the barrier layers. It is seen that the value of the valence-band offset, to within rather large errors, apparently remains remarkably constant, between 20 to 50 meV, for manganese concentrations up to 0.25. This in turn means that the partition ratio decreases rather quickly from about 0.4 at a Mn ion concentration of 0.05 to about 0.1 at a concentration of 0.25.

The experimentally determined magnetic-field splittings of the single-particle $(e_1l_1)^{\pm}$ and $(e_1h_1)^{\pm}$ transitions for sample 1 are shown in Fig. 14. These data have been determined from the magnetic splitting of (e_1h_1) and (e_1l_1) excitons at 2 K shown in Fig. 4, and the changes of the exciton binding energies, derived from the $1S/2S$ splittings shown in Fig. 12. It is found that a partition ratio in the range 0.35–0.45 gives reasonable agreement with the (e_1h_1) data; the dotted lines of Fig. 14(a) show the fit to a partition ratio of 0.4. The corresponding value of the valence-band offset is then between 40 and 52 meV. Comparison with other determinations of the partition ratio in Fig. 13 shows that the present value is in the range of other determinations for this value of the Mn ion concentrations.

However, utilizing this same partition ratio gives poor agreement for the magnetic splittings of the (e_1l_1) transition energy as shown by the dotted lines of Fig. 14(b). The basic problem is that the magnetic-field-induced changes in the well depth of the light hole are one-third those of the heavy hole, and this would produce only small splittings in the $(e_1l_1)^{\pm}$ transitions. One possible means of accounting for the $(e_1l_1)^{\pm}$ magnetic-field splittings is to abandon the assumption of a perfect well-barrier interface, and to allow for the possibility that interdiffusion of Mn ions occurs at the heterostructure interface during MBE growth of the multiple-quantum-well structures. We shall examine the consequences of this possibility in the next subsection.

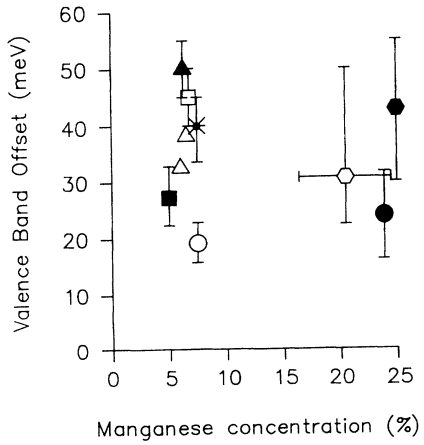

FIG. 13. Values of the valence-band offset, in meV, for $CdTe/Cd_{1-x}Mn_xTe$ heterostructures for different manganese ion concentrations. Data taken as follows: ○, Deleporte *et al.* (Ref. 10); □, Wasiela *et al.* (Ref. 16); ●, Gregory *et al.* (Ref. 17); △, Heimbrodt *et al.* (Ref. 18); ○, Kuhn-Heinrich *et al.* (Ref. 19); ●, Chang *et al.* (Ref. 20); ■, Wasiela *et al.* (Ref. 21); ▲, Halsall *et al.* (Ref. 22); and *, present work.

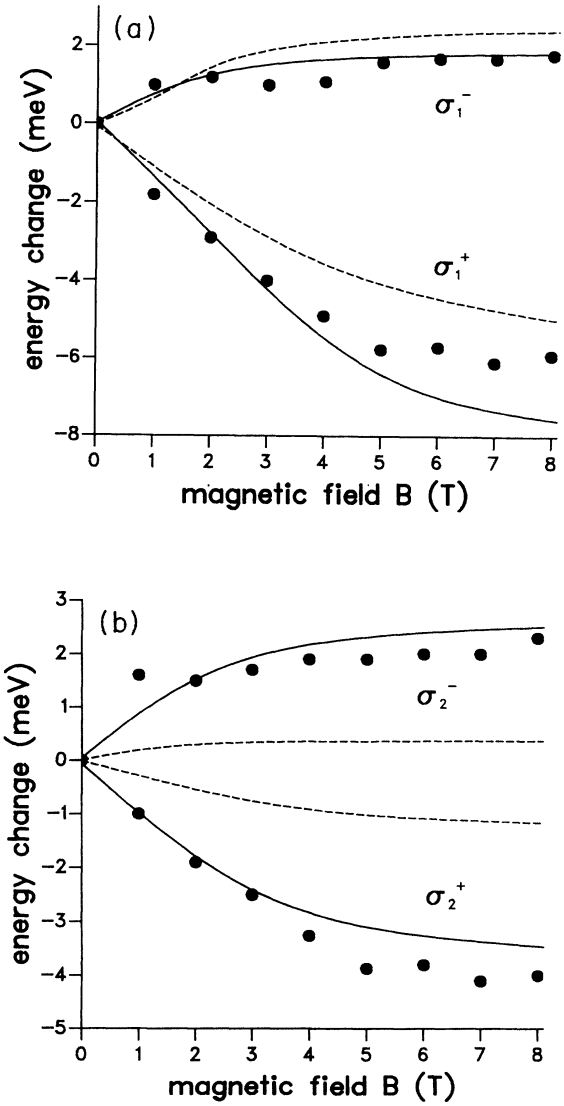

FIG. 14. Single-particle energies for (a) the $(e_1h_1)^{\pm}$ transitions, and (b) $(e_1l_1)^{\pm}$ transitions for sample 1. The data points were found from the observed splittings of the corresponding excitons, Fig. 4, after correction for the change with the exciton binding energies, which were deduced from Fig. 12 assuming a $1S/2S$ binding-energy ratio of 5, as indicated by theoretical calculations of the binding energies (Sec. IV C). The curves are calculated from the envelope-function approximation, with a partition ratio of 0.4. The solid and broken curves are calculated with and without interface potentials, as detailed in the text.

E. Interface diffusion of magnetic ions

The extent of interdiffusion will depend markedly on sample-growth temperature and growth time and, if appreciable diffusion occurs, it will change the shape of the confining potentials and lead to changes of particle-confinement energies which will affect differently the light- and heavy-hole states. To simulate the diffusion, model calculations have been carried out of the diffusion profile, in which the shape of the confining potential was represented by the erf function with a diffusion length $l_d = 2(Dt)^{1/2}$, where D is the diffusion constant and t is the time. Under an applied magnetic field, the shape of the confining potential changes appreciably since the magnetically induced change of the band gap does not vary linearly with the magnetic-ion concentration. To model these changes it was assumed that the conduction- and valence-band edges followed the modified Brillouin function given by Eq. (1), where the empirical parameters $S(x)$ and $T(x)$ depend on the magnetic-ion concentration. Different values of $S(x)$ and $T(x)$ were taken across the diffusion profile from the data of Ref. 8. The ground-state electron and hole energies in the diffusion profile were found by numerical integration of the Schrodinger equation using the shooting technique,[23] assuming the effective masses of Sec. III and a partition ratio of the band offset of 0.4. Figure 15 shows the changes in the confining-potential profile in a magnetic field, while Fig. 16 shows the predicted saturated magnetic-field splitting of the single-particle $(e_1h_1)^{\pm}$ and $(e_1l_1)^{\pm}$ transitions for sample 1, assuming different diffusion lengths. The calculations show that diffusion of magnetic ions across the interface would lead to increased splitting of both the $(e_1l_1)^{\pm}$ and $(e_1h_1)^{\pm}$ transitions, but that the increase would be much more pronounced for the (e_1h_1) transition than for (e_1l_1).

Samples 1 and 2 were both grown at a temperature of 230 °C over a period of approximately 30 min. The effect of diffusion in these samples can be estimated by taking a diffusion constant for Mn ions in CdTe at this temperature to be 3×10^{-8} Å^{2}s^{-1}, a value we have extrapolated from higher-temperature data.[24] This gives an estimated diffusion length of $\sim10^{-2}$ Å. It is therefore clear from Fig. 16 that the effect of this degree of diffusion on the magnetic-field splitting of the $(e_1h_1)^{\pm}$ and $(e_1l_1)^{\pm}$ transitions will be negligible, and that interdiffusion in our samples is unlikely to have affected the observed magnetic-field splittings. Furthermore, the calculations show that even if appreciable diffusion did occur, it would have a much more marked influence on the $(e_1h_1)^{\pm}$ splittings than on the $(e_1l_1)^{\pm}$ splittings. Since we can already account satisfactorily for the $(e_1h_1)^{\pm}$ splittings it is clear that we cannot explain the large splittings observed for $(e_1l_1)^{\pm}$ states by involving interface diffusion. However, we will show in the next subsection that we can account for our results by invoking the concept of interface potentials.

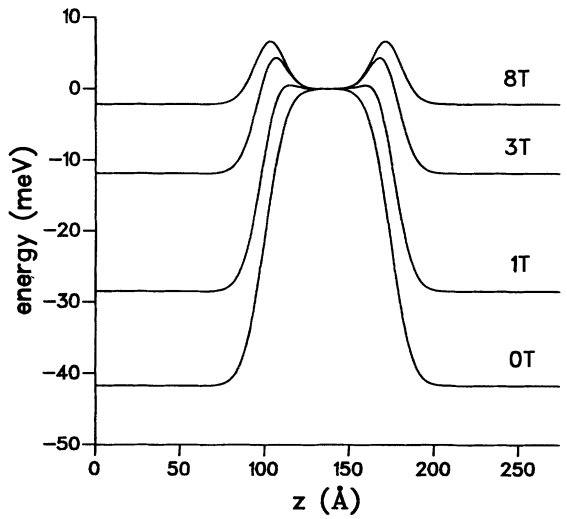

FIG. 15. Change in shape of the heavy-hole potential for a $CdTe/Cd_{1-x}Mn_xTe$ single quantum well with $x = 0.075$, as a function of magnetic field, assuming a diffusion length of 50 Å^2 for the magnetic ions into the well.

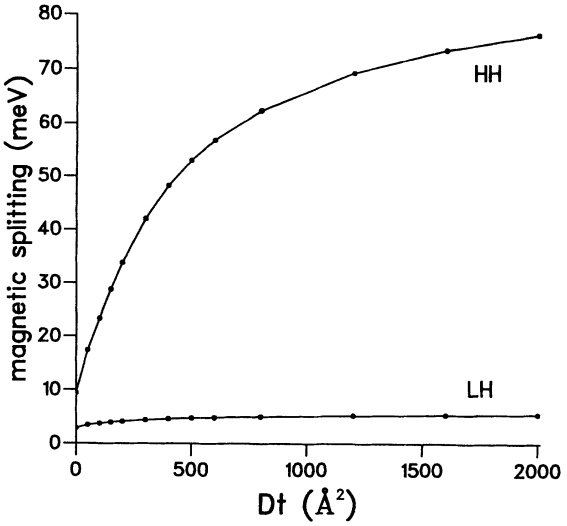

FIG. 16. Calculated splitting of the single-particle $(e_1h_1)^{\pm}$ states, marked HH, and the $(e_1l_1)^{\pm}$ marked LH, as a function of diffusion length L_d^2 ($=Dt$) for single quantum wells as depicted in Fig. 15. A partition ratio of 0.4 was used throughout.

F. Interface potentials

One of the assumptions traditionally employed in the description of quantum-well structures is that the effective one-electron potential "seen" by a free carrier in, say, a barrier, is that appropriate to the bulk material. However, barriers in quantum-well systems are of finite size, and, in particular, translational invariance is lost at the well-barrier interface. The significance of this is that if we denote the effective one-electron potential in a quantum-well structure by $V(r)$, and the corresponding value for the bulk material by $V_0(r)$, then we can write

$$V(\underline{r}) = V(\underline{r}) + V_0(\underline{r}) - V_0(\underline{r}) = V_0(\underline{r}) + V'(\underline{r}) ,$$

where

$$V'(\underline{r}) = V(\underline{r}) - V_0(\underline{r})$$

can be regarded as a perturbation on the bulk one-electron potential $V_0(r)$. In a barrier comprised of N monolayers $V'(\underline{r})$ might, to a good approximation, be zero for $(N-2)$ of the monolayers but the loss of translational symmetry ensures that it *cannot* vanish in the 1-ML region adjacent to the interface. It is thus clear that in any multiple-quantum-well system the loss of translational symmetry at a well-barrier interface implies that $V'(r)$ is nonvanishing in at least one (or more) ML region adjacent to such interfaces. This will remain true, even if the interfaces are perfectly abrupt on an atomic scale. Clearly any surface roughness effects resulting from the growth conditions will only add to this basic feature. We refer to the sum total of such effects, $V'(\underline{r})$, as interface potentials.

With particular reference to the $CdTe/Cd_{1-x}Mn_xTe$ system, we note that one of the essential features is the strong interaction between the charge carriers and the magnetic ions. This is characterized by the parameters $N_0\alpha$ ($\sim$220 meV) and $N_0\beta$ ($\sim$880 meV) describing the exchange interactions between the carriers and the magnetic ions.[8] It is clear that the magnetic Mn^{2+} ions in a barrier next to an interface (with a CdTe well) will experience a different magnetic environment from those further away from the interface. This means, as has been pointed out by several authors,[25,26] that the associated parameters $(N_0\alpha)'$ and $(N_0\beta)'$ of the exchange interaction between the charge carriers and the magnetic (Mn^{2+}) ions may differ from those appropriate to the bulk. In addition, surface roughness effects may result in fluctuations in the number of magnetic ions at least 1 ML on either side of the interface. The sum total of these effects is that the interface potential (which may exist over 1 or 2 ML only) has the form

$$V'(r)=V_A+V_S\ ,$$

where V_A is a one-electron (spin independent) potential, whereas V_S is a spin-dependent potential, i.e., it varies with the magnetic field and has a Brillouin-type dependence. We have already described various effects resulting from these interface potentials.[27] What we wish to demonstrate here is that the existence of such interface potentials can account for an apparent discrepancy in the observed zero-field energy separation of the (e_1h_1) and (e_1l_1) excitons and the anomalously large magnetic-field splittings of the $(e_1l_1)^{\pm}$ transitions. To this end we note that the matrix elements of the potential V_A will be different for the heavy- and light-hole states. Hence, any differences between the experimental value of the one-electron zero-field energies associated with the heavy- and light-hole states compared with the theoretical values expected on the basis of a perfect quantum well having a partition ratio of 0.4, can be assigned to the matrix elements of the potential V_A. Utilizing the experimental values for the exciton binding energies, together with the observed zero-field energy separation of the light- and heavy-hole exciton states, enables the one-electron energy-level separation of the light- and heavy-hole states to be determined. When the latter are compared with those calculated on the basis of an offset ratio of 0.4 it is found that, allowing for experimental errors, the theoretical energy separation is always too high by an amount lying in the range 2–5 meV. It can be readily shown that the matrix elements over the complete structure of the potential V_A for the heavy- and light-hole states differ by $\frac{2}{3}(V_2-V_1)$, where (employing standard notation for the p-type Bloch state of the valence band)

$$V_1=\langle X|V_A|X\rangle=\langle Y|V_A|Y\rangle$$

and

$$V_2=\langle Z|V_A|Z\rangle\ .$$

Hence, in order to account for the observed discrepancies of 2–5 meV requires that (V_2-V_1) is several meV. This in turn means that, as a minimum, $V_2(\sim V_1)$ must be several meV. These matrix elements of V_A have been averaged over the whole quantum-well structure (i.e., 76 ML per period). If, however, V_A exists in about 4 ML only (i.e., within 2 ML adjacent to each interface), then the matrix element of V_A will be about 19 times several meV for a sample such as sample 1. This simply serves to show that, in effect, V_A is a deep, short-range potential.

We consider next the spin-dependent (i.e., magnetic-field dependent) part V_S. Again V_A is assumed to be restricted to only approximately 1 ML on each side of the interface. When a magnetic field is applied the height of the magnetic barrier changes. If $V'(r)$ did not exist, the latter would be uniform across the whole barrier region. However, in the 1-ML region adjacent to the interface the number of free paramagnetic spins could differ from those of the bulk.[21] Similarly, the value of the spin-exchange coupling parameters $N_0\alpha$ (for electrons) and $N_0\beta$ (for holes) could differ from those of the bulk.[25,26] These two effects alone could combine to make the net magnetic response of the ML adjacent to the interface different from the rest of the barrier. *A priori* it is not known whether the net magnetic response of the ML in the conduction and valence bands will be greater or less than that in the rest of the barrier. If it is the former, then, relative to the rest of the barrier, we will have a 1-ML-thick potential well in the conduction band (if the latter decreases overall in a magnetic field) and a 1-ML potential barrier for the case where the ML decreases less. Appropriate modifications need to be made for the case where the barrier potential increases overall in a magnetic field.

We have been able to fit the observed magnetic-field splitting of the light-hole state by assuming that the magnetic response of the conduction band over the 1-ML region was less than the rest of the barrier, while the magnetic response of the valence band was greater than the rest of the barrier for the ML region. The fits obtained in this way, for the magnetic splittings of the $(e_1h_1)^{\pm}$ and $(e_1l_1)^{\pm}$ states, are shown by the solid curves in Fig. 14. While the introduction of these interface potentials does not have a great influence on the overall splitting of the heavy-hole state, relative to that which occurred assuming a perfect interface, the magnetic-field splitting of the light-hole exciton is a more sensitive probe of the ex-

istence of these interface potentials. This observation indicates that all of the samples we have studied have interface potentials present, since in all of them the magnetic-field splitting of the light-hole state is anomalously large in comparison with that expected on the basis of the observed splitting of the heavy-hole state.

V. CONCLUSION

Magneto-optical experiments have been carried out on a series of $CdTe/Cd_{1-x}Mn_xTe$ MQW's. These samples are of high quality, as evidence by the half-width of the PL, PLE, and DCXRD lines and exhibit some degree of both large- and small-scale interface disorder (as compared with the exciton diameter, ~ 140 Å). As a result of observing both $1S$ and $2S$ transitions associated with both the heavy-hole (e_1h_1) and light-hole (e_1l_1) exciton states, we have been able to show that the binding energies are increased appreciably from their three-dimensional bulk values, and that they change only slightly in magnetic fields that are sufficiently high to almost completely saturate the magnetization of the $Cd_{1-x}Mn_xTe$ barrier layers. These same observations, together with negligible changes in the observed oscillator strengths, show that in these quantum-well structures there is no evidence for a magnetic-field-induced type-II transition of one spin component of the heavy-hole valence band. This in turn suggests that the partition ratio probably exceeds 0.35. In fact, all of our observations are consistent with a partition ratio of between 0.35 and 0.45. Calculations of the exciton binding energies have been made with a variational technique, but to obtain agreement between the calculated and observed values would require a change in the Luttinger parameters appropriate to the bulk material and/or utilization of a frequency-dependent dielectric constant. Similarly, the observed zero-field energy and the magnetic-field splitting of the light-hole state can only be accounted for by introducing interface potentials.

ACKNOWLEDGMENTS

We wish to thank the Science and Engineering Research Council, U.K., and the Procurement Executive, Ministry of Defence, for financial support of this work. Also we thank the SERC and the University of Hull for grants to S.R.J. and T.S., respectively.

[1] *Physics and Chemistry of II-VI Compounds,* edited by M. Avon and J. S. Prener (North-Holland, Amsterdam, 1967), Chap. 7.
[2] U. Heim and P. Hiessinger, Phys. Status Solidi B **66**, 461 (1974).
[3] G. M. Williams, A. G. Cullis, C. R. Whitehouse, D. E. Ashenford, and B. Lunn, Appl. Phys. Lett. **55**, 1303 (1989).
[4] D. R. T. Zahn, T. D. Golding, K. J. Mackay, T. Eickhoff, J. Geurts, J. H. Dinan, W. Richter, and R. H. Williams, Appl. Surf. Sci. **41/42**, 497 (1989).
[5] P. J. Dean, G. M. Williams, and G. Blackmore, J. Phys. D **17**, 2291 (1984).
[6] J. C. Hansel and G. Feher, Phys. Rev. **129**, 1041 (1963).
[7] A. Twadoski, M. Nawrochi, and J. Ginter, Phys. Status Solidi B **96**, 497 (1979).
[8] J. A. Gaj, R. Planel, and G. Fishman, Solid State Commun. **29**, 435 (1979).
[9] P. Peyla, A. Wasiela, Y. Merle d'Aubigné, D. E. Ashenford, and B. Lunn, Phys. Rev. B **47**, 3783 (1993).
[10] E. Deleporte, J. M. Berroir, J. M. Bastard, C. Delalande, J. M. Hong, and L. L. Chang, Superlatt. Microstruct. **8**, 171 (1990).
[11] C. P. Hilton, W. E. Hagston, and J. E. Nicholls, J. Phys. A **25**, 2395 (1992).
[12] C. P. Hilton, J. Goodwin, P. Harrison, and W. E. Hagston, J. Phys. A **25**, 5365 (1992).
[13] Le Si Dang, G. Neu, and R. Romestain, Solid State Commun. **44**, 1187 (1982).
[14] P. Harrison, J. Goodwin, and W. E. Hagston, Phys. Rev. B **46**, 12 377 (1992).
[15] B. K. Ridley, *Quantum Processes in Semiconductors* (Clarendon, Oxford, 1988), p. 62.
[16] A. Wasiela, Y. Merle d'Aubigné, J. E. Nicholls, D. E. Ashenford, and B. Lunn, Solid State Commun. **76**, 263 (1990).
[17] T. J. Gregory, C. P. Hilton, J. E. Nicholls, W. E. Hagston, J. J. Davies, B. Lunn, and D. E. Ashenford, J. Cryst. Growth **101**, 594 (1990).
[18] W. Heimbrodt, O. Goede, H.-E. Gumlich, H. Hoffmann, U. Stutenbäumer, B. Lunn, and D. E. Ashenford, J. Lumin. **48 & 49**, 750 (1991).
[19] B. Kuhn-Heinrich, W. Ossau, M. Popp, A. Wang, and G. Landwehr, in *The Physics of Semiconductors,* edited by Ping Jiang and Hon-Zhi Zeng (World Scientific, Singapore, 1992), p. 923.
[20] S.-K. Chang, A. V. Nurmikko, J.-W. Wu, L. A. Kolodziejski, and R. L. Gunshor, Phys. Rev. B **37**, 1191 (1988).
[21] A. Wasiela, P. Peyla, Y. Merle d'Aubigné, J. E. Nicholls, D. E. Ashenford, and B. Lunn, Semicond. Sci. Technol. **7**, 571 (1992).
[22] M. P. Halsall, D. Wolverson, J. J. Davies, D. E. Ashenford, and B. Lunn, Solid State Commun. **86**, 15 (1993).
[23] J. P. Killingbeck, *Microcomputer Algorithms: Action from Algebra* (Hilger, Bristol, 1992).
[24] N. Y. Jamil, Ph.D. thesis, University of Hull, 1990.
[25] M. Kohl, M. R. Freeman, J. M. Hong, and D. D. Anschalom, Phys. Rev. B **43**, 2431 (1991).
[26] D. R. Yakovlev, Adv. Solid State Phys. **32**, 251 (1992).
[27] T. Stirner, P. Harrison, W. E. Hagston, and J. P. Goodwin, J. Appl. Phys. **73**, 5081 (1993).